8th EnvImeko - IMEKO TC19 Symposium on Environmental Instrumentation and Measurements
October 29-30, 2019, Sfax, Tunisia

Electrochemical Characteristic of Interdigital Electrodes Supercapacitors for Embedded Electronics

Marwa Gassab[a,b], Achref Chebil[a,b], Chérif Dridi[a,*]
[a] NANOMISENE Laboratory, LR16CRMN01, Center for Research on Microelectronics and Nanotechnology CRMN of Technopark of Sousse B.P. 334, Sahloul 4034, Sousse, Tunisia
[b] University of Sousse, High School of Sciences and Technology of Hammam Sousse, Tunisia
*dridi2@yahoo.fr

***Abstract*—Micro-supercapacitors (MSCs) are drawing more and more attention in the field of energy storage devices due to their distinct advantages such as their high power density, good electrochemical performances and long maintenance-free lifetime. In this work, a simulative approach (based on FEM (finite element method)) was employed to investigate the interplay of architecture between the geometric parameters for different electrodes number, length and width of an interdigitated structure. Cyclic voltammetry (CV) have been numerically calculated showing the maximum current response for optimized geometry parameters (length= 6500 µm, 16 electrodes width= 200 µm) of about 92 mA/cm². All the results demonstrate that this kind of micro-supercapacitor is a promote candidate that can be used in future autonomous systems.**

***Keywords*— simulation, cyclic voltammetry, interdigital electrode, micro-supercapacitor (MSC)**

I. INTRODUCTION

The global warming and the excessive use of fossil energies have come out with serious issues and problems affecting our daily lives especially for the increasing demand for energy sources. The use of renewable energy as a green source of energy is very attractive [1]. However, these types of energy are not steady they need to be stored. Different storage devices have been investigated and put forward such as fuel cells, batteries and supercapacitors [2]–[5]. The latter possess significant advantages compared to other energy storage approaches due to its high energy density, high-power delivery rates and its long life cycle [6]. This power source can be integrated into different applications like healthcare devices, smart electronics, and different kinds of sensors providing them the required power [7].

Micro-supercapacitor (MSC) also known as an electrochemical capacitor is composed of an electrolyte sandwiched in between two electrodes. A variety of electrode materials can be used in the MSC: conductive polymers, metal oxides, carbon materials such as activated carbon and carbon black [8] which is known as a promising active material due to its high specific surface area [9] low cost, non-toxicity and its eco-friendly impact [10]. Carbon MSC can be fabricated with different methods and strategies like inkjet printing, screen printing, photolithography process [11].

The electrolyte is an essential constituent in supercapacitors and can exist in two forms liquid and solid. The solid-state electrolytes have many advantages such as liquid-leakage free and simple packaging [12]. The Polyvinyl alcohol (PVA) is a biocompatible polymer mainly used as a gel host polymer mixed with liquid electrolyte (aqueous, organic, ionic) [13], [14]. The interdigitated configuration is especially used in the micro-scale for their easy integration with other circuitry on a chip which allows electrical connection in the same plane [11]. This explains the importance of the optimization of the architecture of the MSC to conserve space availability in the microchip and the simple integration in microelectronics.

In the following, we target to maximize the electrical output current by the simulation of CV for different micro-supercapacitors by optimizing the geometric architecture to obtain high performance of the micro storage devices.

II. METHODOLOGY

A. Design of interdigitated supercapacitor

In this study, the 2D structure is designed to construct a planar supercapacitor, in which each negative and positive electrode consists of several sub-electrodes that are interdigitally arranged separated by an interspace in the same plane.

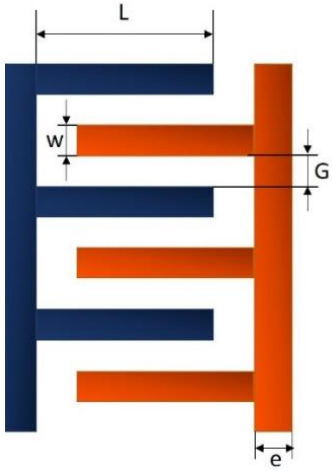

Fig. 1. The architecture geometry of the studied interdigitated supercapacitor

The schematic illustration of the electrodes architecture is illustrated in Fig. 1. The MSC was constructed of gold current collector and carbon black as electrode material. This

structure includes solid-state polymer electrolyte based on PVA/H_2SO_4 set in the domain between the fingers.

To study the influence of geometric parameters of the interdigitated architecture, different structures were designed and simulated using FEM. The interspace between the fingers (gap), the length (L) and the two edges of fingers (e) were kept constant to 4500µm and 300µm respectively. Therefore, the working area will be constant. The number of sub-electrodes (N) and the width of fingers (w) were modified as detailed in the Table1. The total surface area is assessed to be 44.66 mm² cited in the reference [15] and calculated by the following formulation:

$$A=W*(w+G)*N \quad (1)$$

where A is the total surface area, W is the sum of the pads (the length, the gap and the two edges), w is the width of fingers, G is the gap and N is the total number of fingers.

Table 1. Dimensions of the studied MSC with different number of fingers

Number of fingers	4	8	12	16
Length (µm)	4500	4500	4500	4500
Gap (µm)	300	300	300	300
Width (µm)	1700	700	366.6	200
Edge (µm)	391.25	391.25	391.25	391.25
Surface Area (mm²)	44.66	44.66	44.66	44.66

For this work, two modules were implemented, the Transport of Diluted Species interface for chemical species diffusion described by Fick's second equation [16] and the secondary current distribution generated by Butler-Volmer kinetics from which the output current in the working electrode will be calculated [16]. The potential is defined as a linear triangular waveform built using a predefined function 1[V]*Scan (t/1[s])-0.5[V].

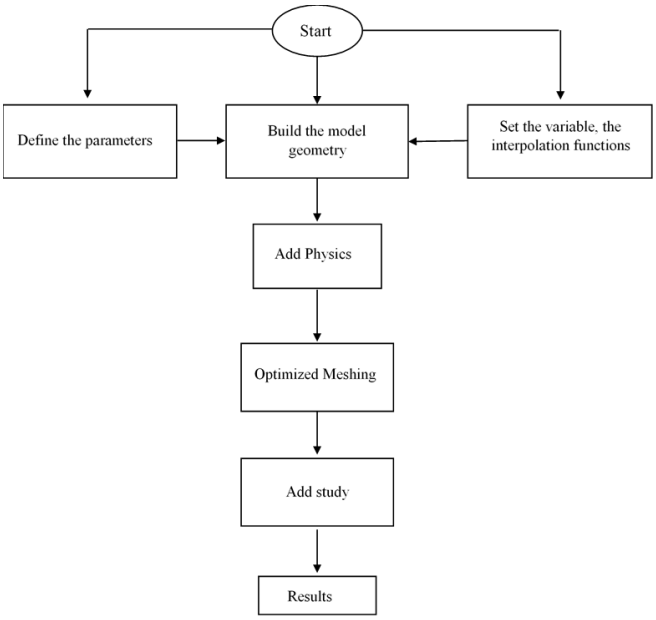

Fig. 2. Flow chart of the simulation with finite element method

B. Theory

The electrode reaction is based on the electrochemical process in which the oxidized and reduced species take part in a single electron transfer process at the electrode-electrolyte interface.

$$O+e- \underset{k_{red}}{\overset{k_{ox}}{\rightleftharpoons}} R \quad (2)$$

These two reactions are characterized by the rate constants k_{ox} and k_{red} (cm/s) expressed as follows:

$$k_{ox}=k^0 e^{\left[\frac{\alpha F(E-E_0)}{RT}\right]} \quad (3)$$

$$k_{red}=k^0 e^{\left[-\frac{(1-\alpha)F(E-E_0)}{RT}\right]} \quad (4)$$

where α is the transfer coefficient called also symmetry factors equal to 0.5 due to the symmetry reaction; E is the electric potential; E_0 is the potential reference equal to 0V; k^0 is the standard electron-transfer rate constant; R molar gas constant (8.3144 J mol^{-1} K^{-1}); F Faraday constant (96485 C mol^{-1}) and T room temperature .

These constants are also linked to the concentration of species to form the reaction rate for the forward and backward reaction (M s^{-1});

$$r_{ox}=k_{ox}.C_{red} \quad (5)$$

$$r_{red}=k_{red}.C_{ox} \quad (6)$$

Where C_{red} and C_{ox} are the concentration of reduced and oxidized species respectively expressed in $mol.m^{-3}$.

The output current of the cyclic voltammetry generated by the faradic process is as follows:

$$I=i_0(C_{red}e^{\frac{\alpha F}{RT}E}-C_{ox}e^{\frac{-\alpha F}{RT}E}) \quad (7)$$

These outcomes are known generally as the Butler-Volmer formulation of electrode kinetics which describes the charge transfer between the electrode and the electrolyte.

III. RESULTS AND DISCUSSIONS

The use of an appropriate mesh is crucial in the simulation in the finite element method to obtain optimized value. Thus, we used the extremely fine element, which allows the obtention of an accurate solution.

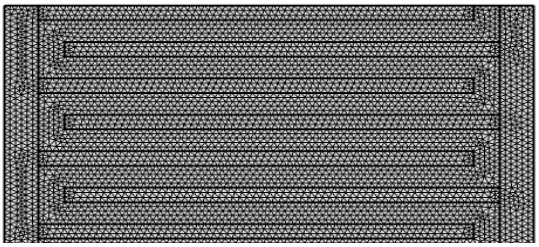

Fig. 3. Visualization of the mesh

In order to study the variation of the surface charge density at the electrode, an electric potential was applied between the electrodes (anode and cathode). Fig. 4 shows that the regular increase in voltage increases the surface charge density at the cathode. A closer perception into the structure shows that the maximum value of the charge density is observed at the edges and the corners due to the mobile charged ion accumulation between the interdigital fingers of the two electrodes.

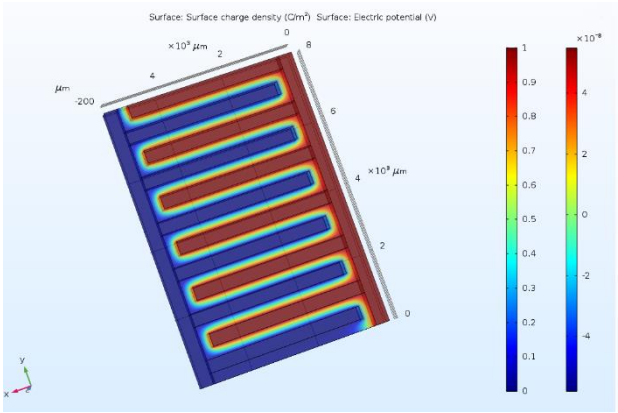

Fig. 4. The surface charge density distribution of the MSC with 12 fingers at an applied potential of 1V

The cyclic voltammetry curves have been simulated by applying a potential range of -0.5V to 0.5 V within the working electrode vs the reference. The current output will flow from the working to the counter electrode. In our case, we used a two-electrode system in the electrochemical cell. The potential was set to 1V referring to the working potential of the H_2SO_4 electrolyte [17]. The cyclic voltammetry defines the faradic current resulted from the chemical reaction and the electron transfer in the electrode-electrolyte interface which can be explained by the oxidation and reduction of species by scanning the potential forward and backward between electrodes.

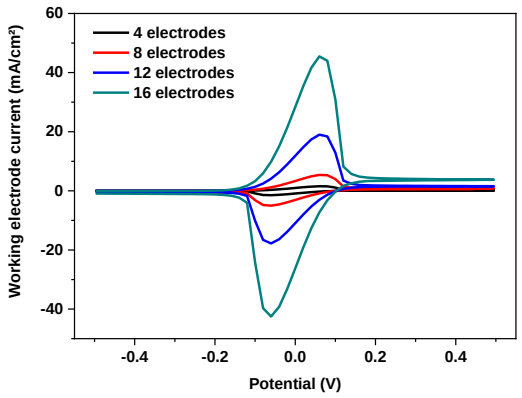

Fig. 5. The evolution of cyclic voltammetry performance of 4, 8, 12, 16 different fingers.

As shown in Fig. 5 the enhancement of potential increases the flowing current, showing the beginning of oxidation and reduction of species of analyte that take place between -0.2V and 0.2V which is explained by the diffusion of ionic species from the electrolyte bulk to the electrode and vice versa. To study the effect of geometry parameters of four supercapacitors were constructed by varying the number of fingers from 4 to 16 and by decreasing the width for each one as detailed in table 1.

It is observed from Fig 5 that the evolution of current is related to the increase of the number of fingers and the decrease of the width. The maximum value of the output current was 45.47 mA/cm² for 16 fingers and 200 µm width. The width of the electrodes shortens the pathway for ion diffusion from the electrolyte to the electrode material and the number of fingers can enhance the electrochemical surface area as observed in the reference [18].

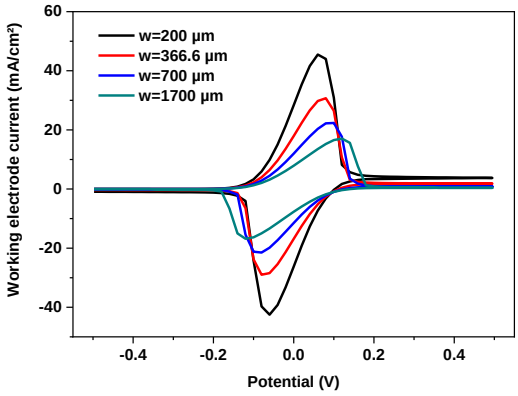

Fig. 6. The evolution of cyclic voltammetry of 16 electrodes supercapacitor for various values of width

In Fig. 6, the number of electrodes was fixed to 16 and the width studied values were 1700 µm, 700 µm, 366.6 µm, 200 µm. The voltammograms in Fig.6 shows that the increase of width reduces the available area for the electrolyte, which limits the faradic reactions at the surface of the electrode.

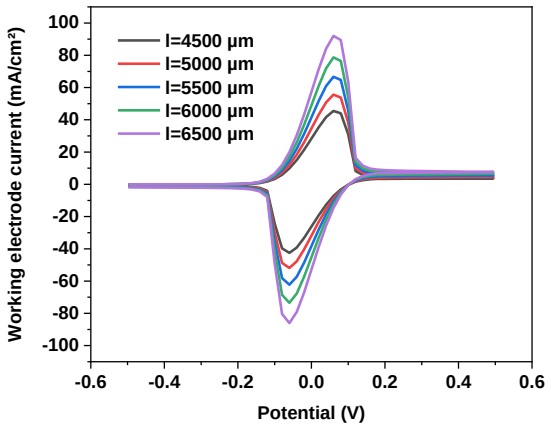

Fig. 7. The evolution of cyclic voltammetry of 16 electrodes supercapacitor for various values of length

Fig. 7 shows that the increase of length gives the highest current in the working electrode. The maximum current value of 92 mA/cm² is achieved for a length of 6500 µm. This is could be explained by the increase of the surface of active material giving rise to more important redox and transport activities at the electrode/electrolyte interface.

IV. Conclusion

This paper presents a numerical simulation of cyclic voltammetry plots for micro-scale supercapacitors. This work is based on a 2D simple design of an interdigitated storage device based on eco-friendly and cost-effective electrode materials. The present simulation of cyclic voltammograms investigates the influence of the architecture in the output current performance.

This method reveals that better performance can be achieved with more interdigital electrodes per unit area and the less width of sub-electrodes.

These results demonstrate and provide an effective approach to optimize and improve the performances of solid-state energy storage devices and provide the energy required for embedded systems.

References

[1] S. Shahzad *et al.*, "Ionic Liquids as Environmentally Benign Electrolytes for High-Performance Supercapacitors," *Glob. Challenges*, vol. 3, no. 1, p. 1800023, Jan. 2019.

[2] C. Santoro, C. Arbizzani, B. Erable, and I. Ieropoulos, "Microbial fuel cells: From fundamentals to applications. A review," *J. Power Sources*, vol. 356, pp. 225–244, Jul. 2017.

[3] J.-M. Tarascon and M. Armand, "Issues and challenges facing rechargeable lithium batteries," in *Materials for Sustainable Energy*, Co-Published with Macmillan Publishers Ltd, UK, 2010, pp. 171–179.

[4] H. Nan, X. Hu, and H. Tian, "Recent advances in perovskite oxides for anion-intercalation supercapacitor: A review," *Mater. Sci. Semicond. Process.*, vol. 94, pp. 35–50, May 2019.

[5] L. Zheng, T. Xing, Y. Ouyang, Y. Wang, and X. Wang, "Core-shell structured MoS2@Mesoporous hollow carbon spheres nanocomposite for supercapacitors applications with enhanced capacitance and energy density," *Electrochim. Acta*, vol. 298, pp. 630–639, Mar. 2019.

[6] X. Feng *et al.*, "All-solid-state planner micro-supercapacitor based on graphene/NiOOH/Ni(OH)2 via mask-free patterning strategy," *J. Power Sources*, vol. 418, pp. 130–137, Apr. 2019.

[7] Y. Lu, Z. Lou, K. Jiang, D. Chen, and G. Shen, "Recent progress of self-powered wearable monitoring systems integrated with microsupercapacitors," *Mater. Today Nano*, vol. 8, p. 100050, Dec. 2019.

[8] A. González, E. Goikolea, J. A. Barrena, and R. Mysyk, "Review on supercapacitors: Technologies and materials," *Renew. Sustain. Energy Rev.*, vol. 58, pp. 1189–1206, May 2016.

[9] P. Kossyrev, "Carbon black supercapacitors employing thin electrodes," *J. Power Sources*, vol. 201, pp. 347–352, Mar. 2012.

[10] X. Ren *et al.*, "Assembly of Mn3O4/carbon Black Composite and Its Supercapacitor Application," *Int. J. Electrochem. Sci*, vol. 11, pp. 5080–5089, 2016.

[11] N. Liu and Y. Gao, "Recent Progress in Micro-Supercapacitors with In-Plane Interdigital Electrode Architecture," *Small*, vol. 13, no. 45, p. 1701989, Dec. 2017.

[12] B. Pal, S. Yang, S. Ramesh, V. Thangadurai, and R. Jose, "Electrolyte selection for supercapacitive devices: A critical review," *Nanoscale Adv.*, vol. 1, no. 10, pp. 3807–3835, 2019.

[13] H. T. T. THANH, P. A. LE, M. D. THI, T. LE QUANG, and T. N. TRINH, "Effect of gel polymer electrolyte based on polyvinyl alcohol/polyethylene oxide blend and sodium salts on the performance of solid-state supercapacitor," *Bull. Mater. Sci.*, vol. 41, no. 6, p. 145, Dec. 2018.

[14] C. Zhong, Y. Deng, W. Hu, J. Qiao, L. Zhang, and J. Zhang, "A review of electrolyte materials and compositions for electrochemical supercapacitors," *Chem. Soc. Rev.*, vol. 44, no. 21, pp. 7484–7539, 2015.

[15] P. Zhang *et al.*, "Zn-Ion Hybrid Micro-Supercapacitors with Ultrahigh Areal Energy Density and Long-Term Durability," *Adv. Mater.*, vol. 31, no. 3, p. 1806005, Jan. 2019.

[16] W. (Waldfried) Plieth, *Electrochemistry for materials science*. Elsevier, 2008.

[17] B. K. Singh, A. Shaikh, S. Badrayyana, D. Mohapatra, R. O. Dusane, and S. Parida, "Nanoporous gold–copper oxide based all-solid-state micro-supercapacitors," *RSC Adv.*, vol. 6, no. 102, pp. 100467–100475, Oct. 2016.

[18] M. F. El-Kady and R. B. Kaner, "Scalable fabrication of high-power graphene micro-supercapacitors for flexible and on-chip energy storage," *Nat. Commun.*, vol. 4, pp. 1475–1479, 2013.